Development of an on-machine vision-based micro depth error measurement method for micro machining

Shih-Ming Wang[1,#], Han-Jen Yu[1] Shih-His Liu[1] and Da-Fan Chen[1]

1Department of Mechanical Engineering, Chang Yuan University, Chang-Li, 32023, Taiwan
Corresponding Author / E-mail: shinming@cycu.edu.tw, TEL: +886-3-265-4340

KEYWORDS : Depth error measurement, Micro-machining, Image re-constructive

The error measurement method was an essential for further enhancing the machining accuracy of a micro machine tool. An on-machine vision-based measurement method that can measure 2-D contouring-/tracking errors of a micro machining process had been previously developed. An on-machine depth-error measurement method was proposed in this study to fulfill the complete 3-D machining errors measurement. The method adopts image re-constructive technology and camera pixel correction to provide non-contact measurement capability. To improve the measurement limits due to the pixel resolution and the filler of view of a CCD, a 2-step measurement method with use of a depth model was developed. Because of the capability of eliminating the shadow effects caused by the tilting light source, the proposed method provides more accurate and reliable measurement results. Sensitivity analysis was conducted to assess the influence of the CCD setup errors on the measurement accuracy for implementation. Experiment was conducted and the results have shown the effectiveness and feasibility of the measurement method.

Manuscript received: January XX, 2011 / Accepted: January XX, 2011

NOMENCLATURE

b = actual depth of the machined side wall of the workpiece
D1 = width of shadow
D2 = idth of the iso-gray level area (distance between upper and lower edges) in the image taken at B1o (B1≠0°)

1. Introduction

Miniaturization has been the development trend of high-tech products. The method for manufacturing the miniaturized components for the high-tech products needs to be accurate and suitable for a variety of materials. The non-MEMS micro manufacturing technology has been recognized as an essential for the manufacturing trend. Micro machining with use of a CNC micro machine tool plays an important role in the non-MEMS micro manufacturing field. An adequate error measurement method integrated with a compensation method is a more effective way to further enhance the machining accuracy for a micro machine tool without increasing too much manufacturing cost.

Up-to-day, not much efforts have been devoted to develop the machining error measurement and compensation method for micro machining. Due to the limit of probe size, the Coordinate Measurement Machine is not adequate for error measurement for micro parts. For the purpose of error compensation, because additional errors could be introduced due to re-installing the workpiece back to the machine, other off-line measurement method is also not adequate for micro part. Thus, a proper error measurement method for micro machining should be with the characteristics of non-contact and on-machine executable. That is, the method should be able to on-machine directly measure the errors from the part. Although the laser vision-based measurement method can provide non-contact and on-machine measurement capability, complexity in installation and expensive cost of the measurement instrument are the drawbacks of the method. Thus, the vision-based measurement method is more feasible for this application.

In the past, because of the expensive cost of instruments and limits in image resolution, machine-vision technology was not extensively applied to all industrial applications. Through continuous improvements, the technology is maturing day by day. In recent years, as PCs have become more powerful and capable in calculation, and resolution of CCD system has been significantly improved, vision-based systems are extensively implemented in many applications [1-3]. Comparing to the measurement methods currently used in precision industry, the advantages of vision-based measurement method include: (1) better efficiency - instead of scanning or point-by-point measurement, it can directly identify the workpiece contour/shape; 2. cost effective; 3. suitable for micro parts (non-contact measurement) ; 4. easy setup. For the application on machining, J. Jurkovic [4] used a CCD camera to obtain high resolution grey-level images of the tool wear projected with a laser vision-based measurement method. The beam pattern was connected to an interface card in a PC, and equipped with image capturing software. Johan Baeten [5] exploited a hybrid vision/force control approach at corners in planar-contour following resulting in a more accurate and faster task execution. The vision system was used for online measurement of the contour and to watch out for corners. Once a corner is detected, a finite-state controller is activated to take the corner in the best conditions. Liangyu Lei [6] utilizes a machine-vision system for inspecting the inner and outer diameters of bearings and realizes a highly-efficient, accurate and reliable inspection method for bearing diameter measurement. P.F. Luo [7] combines a computer-vision, a laser vision-based measurement method, interferometer, and a CMM to form a vision-inspection system that can perform inspection work over a large area. This system was then used to measure the line space on a standard line scale made of glass to verify its defined accuracy. To improve the defined accuracy, methods of locating an edge to sub-pixel resolution and fitting a line to the determined edge points have been investigated. The inspection technique proposed by this paper can be applied to build a two-dimensional inspection system. Kok-Meng Lee [8] offers an alternative design of an optical sensor for simultaneous measurement of three-DOF planar motions. The design begins with the operational principle of a microscopic-surface-based optical. The dual-sensor system, which detects microscopic changes in consecutive images, computes the angular displacement of a moving surface and the instantaneous center of rotational axis.

The methods mentioned above can measure errors for different applications, but not appropriate for on-machine error compensation which can directly improve the machining accuracy. An on-machine image-based measurement method that can measure 2-D contouring-/tracking errors of a miniature workpiece was developed in our previous research [9]. Extending the research, a depth-error measurement method using a 4-degrees-of freedom CCD incorporated with image re-constructive method and a derived depth measurement model was proposed in this paper. With use of the two measurement methods, 3D machining errors of a micro machining process can be measured. When the errors are compensated, the accuracy of the micro machining process can be further improved.

The depth-error measurement method composes of a 4- degrees-of freedom CCD, image re-constructive method, and a derived depth measurement model. To eliminate the shadow effect, an error model and a 2-step measurement procedure were developed. The principle of the measurement method was addressed in section 2. Sensitivity analysis exploring the influence of major system errors on the measurement accuracy was discussed in section 3. In Section 4 the experimental results were discussed. Finally, the conclusion was addressed in section 5.

2. Principle of Measurement Method

To measure the depth of a machined contour such as a slot, two images are taken at two different rotation angles by a CCD (Fig. 1). Based on the two images, the upper and lower edges of the machined side wall in the images are detected by Canny Edge Detection method, and the distance between the two edges (i.e. between Pcp1 to pcp2) is computed (Fig.2). The distance is then substituted into a derived depth measurement model to determine the depth. Finally the measured depth was compared to the theoretical depth to calculate the depth errors. Figure 3 shows the flowchart of the micro depth error measurement method. The measurement processes can be divided into three parts: (1) take images of the machined side wall; (2) detect the iso-gray level area; (3) calculate the micro depth.

2.1 2-step Images Taking

A measurement apparatus (Fig. 4) composing of a CCD, a 4 degree-of-freedom platform, and light source was designed for taking images. The CCD was mounted on the platform. The platform can move along x, y, and z axis with accuracy of 0.01 mm and rotate about y-axis with accuracy of 0.0216^{o}. The specification of the CCD is listed in Table 1.

Before taking the image of the machined side wall (Fig. 1), a coordinate frame $(x, y, z)_{e'}$ is defined at the upper edge of the machined side wall, and $(x, y, z)_f$ is defined as the CCD coordinate frame. ye' axis is perpendicular to the xf-zf plane. The CCD is rotated about yf-axis for $B1^{o}$ to take the first photo for the machined side wall. Then, the CCD is rotated to $(B1+B2)^{o}$ to take the second photo for the machined side wall. The machined side wall will show as an iso-gray level area in the two images.

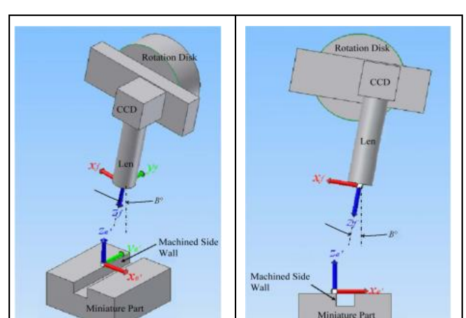

(a)side view (b)front view

Fig.1 Image taken from different locations for depth error measurement

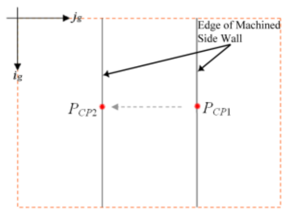

Fig. 2 Distance between upper and lower edges in the image

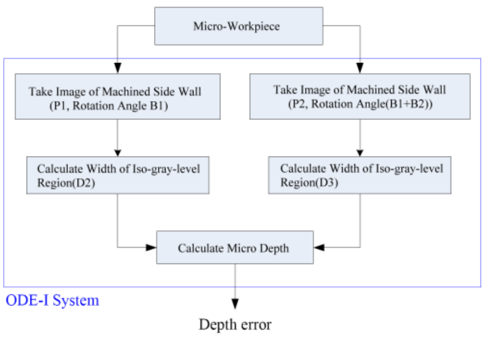

Fig. 3 Flowchart of the micro depth error measurement method

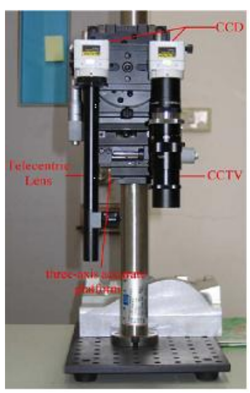

Fig. 4 Apparatus of on-machine micro depth error measurement system

CCD	Sentech Color CCD(P63) Size : 1/3 inch Image size : 752(H) ×582(V)pixel Scan speed : 25 frame per second	
Lens	CCTV Len F: 75mm	Telecentric Len 12X
F.O.V. (Length × Width)	Depends on operation distance	0.30×0.40mm ~5×10^{-7}m/pixel
I/O card	Altair Series Frame Grabber(OVK Framework)	

Table 1 Comparison of measured roughness data

2.2 Detection of The ISO-gray Level Area

To detect the shape of a machined workpiece, the Canny Edge Detection algorithm [10] was adopted to search for the optimal edges of the image. The Canny Edge Detection has better detection results relative to traditional binary methods. The main characteristics of Canny Edge Detection are as follows:

1. Smoothes the image with a Gaussian filter;
2. Computes the gradient magnitude and orientation using 2×2 first-difference approximations for the partial derivatives;
3. Applies nonmaxima suppression to the gradient magnitude;
4. Uses a double thresholding algorithm to detect and link edges.

2.2.1 Gaussian Filter

Let I [i, j] denote the image, the result of convolution with Gaussian smoothing filter is an array of smoothed data,

$$S[i,j] = G[i,j;\sigma] * I[i,j] \tag{2}$$

where σ is the spread of the Gaussian and controls the degree of smoothing.

For digital images, the derivatives are approximated by differences equation. S[i, j] can be calculated by the 2×2 first-difference approximations to produce Gx and Gy as below,

$$G_x \approx (-S[i,j] + S[i,j+1] - S[i+1,j] + S[i+1,j+1])/2 \tag{3}$$

$$G_y \approx (S[i,j] + S[i,j+1] - S[i+1,j] - S[i+1,j+1])/2 \tag{4}$$

The magnitude and orientation of the gradient can be computed from the standard formulas for rectangular-to-polar conversion,

$$M[i,j] = \sqrt{G_x^2 + G_y^2} \tag{5}$$

$$\theta[i,j] = a\tan(G_y, G_x) \tag{6}$$

As to this research, the characteristic lies in measuring the shape of milling, so the choice for σ is quite important. When σ is chosen too small, disorderly signals would be created in the detection result so that the actual edge of milling is unable to be judged, but when σ is too large, the edge of the milling would be filtered so that a discontinuous situation is created. Properly choosing σ is the first step for edge detection. For the material used in this study, it is found that the proper value of σ lies between 8 and 12.

2.2.2 Nonmaxima Suppression

To identify edges, nonmaxima suppression is used to get the greatest local points of the magnitude array. The nonmaxima suppression thins broad ranges of potential line pixels into ridges that are only one pixel wide. This helps the segmentation process generate a line segment at the edge.

The algorithm begins by reducing the angle of the gradient θ[i, j] to one of the four sectors,

$$\zeta[i,j] = \begin{cases} 0 & \text{if} \quad \theta \in [-\Delta\theta, \Delta\theta] \quad \text{or} \quad [135^\circ+\Delta\theta, 225^\circ-\Delta\theta] \\ 1 & \text{if} \quad \theta \in [\Delta\theta, 90^\circ-\Delta\theta] \quad \text{or} \quad [180^\circ+\Delta\theta, 270^\circ-\Delta\theta] \\ 2 & \text{if} \quad \theta \in [45^\circ+\Delta\theta, 135^\circ-\Delta\theta] \quad \text{or} \quad [225^\circ+\Delta\theta, 315^\circ-\Delta\theta] \\ 3 & \text{if} \quad \theta \in [90^\circ+\Delta\theta, 180^\circ-\Delta\theta] \quad \text{or} \quad [270^\circ+\Delta\theta, -\Delta\theta] \end{cases} \tag{7}$$

where Δθ = 22.5°.

At each point, the center element M[i, j] is compared with its two neighbors along the line of the gradient that is given by the sector value ζ[i, j] at the center. If M[i,j] at the center is not greater than one of the neighboring magnitudes that is along the gradient line, then M[i, j] is set to zero. The values for the height of the ridges are retained in the nonmaxima-suppressed magnitude. The nonmaxima suppression process is,

$$N[i,j] = nms(M[i,j], \zeta[i,j]) \tag{8}$$

The non-zero values in N[i, j] correspond to the amount of contrast in the image intensity. Although the smoothing is performed as the first step in edge detection, the nonmaxima-suppressed magnitude image N[i, j] will contain many false edge segments caused by noise and texture. The contrast of the false edge segments is small.

2.2.3 Double Threshold Algorithm

Although smoothing is performed in the Gaussian smoothing, the nonmaxima-suppressed magnitude M[i,j] would still contain many false edge segments that are caused by noise and refined texture. However, the contrast of the false edge segments is small.

These false edge segments in the nonmaxima-suppressed gradient magnitude should be reduced. The typical procedure is to apply a threshold to M[i, j]. The values of M[i, j] below the threshold are adjusted to zero. After the application of the threshold to the nonmaxima-suppressed magnitude, the edges of the image are obtained. However, using the right threshold value in this method is difficult. There may still be some false edges if the threshold is too low or some edges may be missing if the threshold is too high. The effective threshold scheme is to use two thresholds.

In order to overcome the problem, two threshold values, T1 and T2 (with T2>T1) are applied. With these threshold values, two threshold edge images E1 and E2 are generated. The image E2 has gaps in the contours, but contains less false edges. With the double threshold algorithm, the edges in E2 are connected to contours. When it approaches the end of a contour, the edges of E1 can be linked into the contours by the locations of the 8-neighbours. The algorithm continues until the gaps in the contours in E2 have been joined.

2.3 Calculation of micro depth

In order to avoid the light reflection effect, light source usually will not be set perpendicularly to workpiece surface. However, tilting light source will generate shadow that affects the measurement accuracy. As shown in Fig. 5(a), when the light source projects the upper edge of the side cutting surface to the bottom surface, if CCD takes image from right up corner at rotation angle B1, the distance between upper and lower edges of the side cutting surface is D2. Different tilting angle of light source gives different width of shadow that gives different value of D2. According to the geometric relationship, when CCD rotates B1^o, the actual depth b can be expressed as

$$b = D1 \times Tan(B1) + \frac{D2 - \dfrac{D1}{Cos(B1)}}{Sin(B1)} \tag{9}$$

Where

b : actual depth of the machined side wall of the workpiece

D1 : width of shadow

D2 : width of the iso-gray level area (distance between upper and lower edges) in the image taken at B1^o (B1≠0°)

When the CCD rotates to the orientation (B1+B2)^o (Fig. 5(b)), the actual depth b can be expressed as

$$b = D1 \times Tan(B1+B2) + \frac{D3 - \dfrac{D1}{Cos(B1+B2)}}{Sin(B1+B2)} \tag{10}$$

Where

D3 : width of the iso-gray level area (distance between upper and lower edges) in the image taken at (B1+B2)^o (B1+B2≠0°)

Based on Eq. (9) and (10), D1 can be solved as

$$D1 = Csc(B2) \times (D2 \times Sin(B1+B2) - D3 \times Sin(B1)) \tag{11}$$

Substituting (11) into (9) or (10), the actual depth *b* can be solved as

$$b = (D3 \times Cos(B1) - D2 \times Cos(B1+B2)) \times Csc(B2) \tag{12}$$

With use of Eq. (11) and (12), when CCD takes photos of a machined contour from two orientations (B1^o、(B1+B2)^o), the actual depth of the machined micro contour can be determined. After comparing the actual depth to the nominal depth, the machining depth error can be determined.

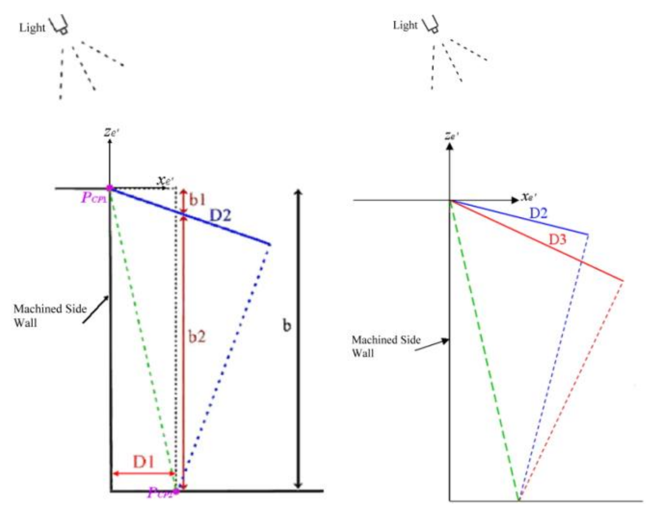

(a) shadow effect with rotation angle B1 (b) width of the iso-gray level area at angles (B1) & (B1+B2)

Fig.5 Illustration of shadow effect and 2-step measurement algorithm

3. Sensitivity Analysis

Manufacturing error of the platform and alignment error of the camera could cause rotation errors ΔC (about z-axis) between the two coordinate frames $(x, y, z)^{e'}$ and $(x, y, z)^{f}$ (Fig. 6). The error will deviate of the measurement point from P_{CP2} to P'_{CP2} (Fig.7) and cause measurement errors. With the derivation of coordinate transformation matrix (between rotation angle B1 and (B1+B2)) and numerical analysis, the influence of the rotation angle error ΔC on the measurement accuracy was investigated.

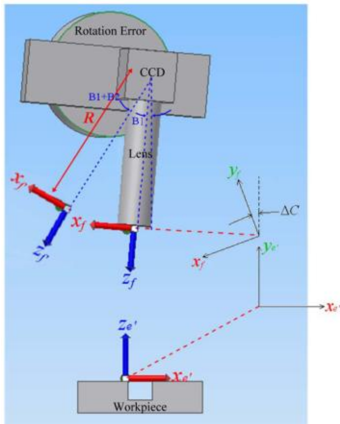

Fig.6 Camera with rotation error ΔC

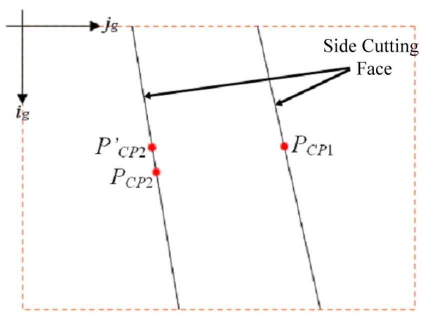

Fig.7 Deviation of side cutting dace P_{CP2} due to ΔC

A workpiece reference coordinate frame $(x, y, z)^{e'}$ was assigned on the side cutting edge, and a camera coordinate frame $(x, y, z)^{f}$ was assigned when the camera was at rotation angle B1. Besides, a pixel coordinate frame $(i, j)^{g}$ was also assigned on the photo. After taking photos at different angles B1 and (B1+B2), the measurement point on the upper and lower edges were first transformed with respect to (w.r.t.) the camera coordinate frame $(x, y, z)^{f}$, and then w.r.t. the pixel coordinate frame $(i, j)^{g}$. Thus, the transformation matrix between camera coordinate frame and the pixel coordinate frame at rotation angles B1 and (B1+B2) were derived. After the coordinate transformation, the actual depth b can be expressed as function of the orientation of the camera. When the camera orientation error ΔC exits, the actual depth b becomes will exit.

$$b' = b + (\Delta b)_{\Delta C} \tag{13}$$

where $(\Delta b)_{\Delta C}$ represents the depth measurement error, and b' represents the actual depth measurement.

When a workpiece has machined depth of 1 mm, the coordinates of the measurement point on the upper edge w.r.t. workpiece coordinate frame is (0, 0, 0) and the coordinates of the measurement point on the lower edge is (0, 0, -1). Assume the two photos were taken at B1=10° and B2 = 10°, the relationship between ΔC and $(\Delta b)_{\Delta C}$ is

$$(\Delta b)_{\Delta C} = b' - b = -1.94 + 0.984808\sqrt{0.969846(1 + Cos(\Delta C))^2 + Sin(\Delta C)^2} \tag{14}$$

Based on Eq. (14), Fig. 8 shows the variation of depth measurement error $(\Delta b)_{\Delta C}$ due to the changes of ΔC. It was noted that, if ΔC can restricted within ±3°, the measurement error $(\Delta b)_{\Delta C}$ can be controlled within±0.0001 mm.

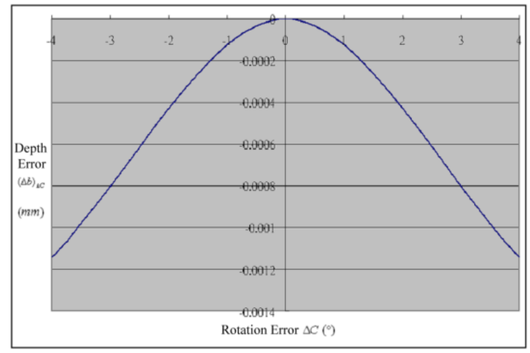

Fig.8 Depth measurement error V.s Rotation error ΔC

Based on Eq. (14), the sensitivity parameter for ΔC is obtained a s

$$\frac{\delta(\Delta b)_{\Delta C}}{\delta \Delta C} = \frac{(-0.955112 + 0.0296956Cos(\Delta C))Sin(\Delta C)}{\sqrt{0.969846 + 1.93969Cos(\Delta C) + 0.969846Cos(\Delta C)^2 + Sin(\Delta C)^2}} \tag{15}$$

According to Eq.(15), when ΔC is within ±4°, the variation of $\frac{\delta(\Delta b)_{\Delta C}}{\delta \Delta C}$ can be simulated as shown in Fig. 9.

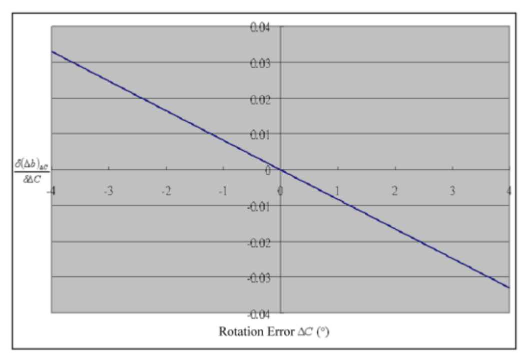

Fig.9 $\frac{\delta(\Delta b)_{\Delta C}}{\delta \Delta C}$ V.s ΔC

As it can be seen from Fig. 9, the sensitivity parameter is approximately linear proportional to ΔC. The influence of ΔC on measurement accuracy becomes larger while ΔC is larger. The analysis result is quite consistent with the numerical simulation result.

4. Experiments

Two experiments were conducted to verify the effectiveness of the proposed method.

4.1 Measurement Accuracy Verification

In the experiment, a 0.33 mm-thickness standard gage was measured by the proposed method. The camera pixel resolution for this measurement was set as 0.003 mm/pixel. Table 2 shows the measurement results. The measured depth was 0.3334 mm.

Comparing the measured with nominal depth 0.33 mm, it was noted that the measurement error was 0.0034 mm which is equal to the size of 1 pixel. Because tolerance of ±1 pixel is quite reasonable for image-based measurement, the experiment result has shown the effectiveness of the proposed method. If camera with finer pixel resolution is used, the measurement accuracy can be further enhanced.

Workpiece	Standard thickness gage	
Nominal gage thickness	0.33 mm	
Pixel resolution	Angle B1 6.645°	0.0029 mm/pixel
	Angle(B1+B2) 19.3723°	0.0030 mm/pixel
Measured Depth	0.3334 mm	

Table.2 Results of verification experiment

4.2 Measurement on a Micro Machined Workpiece

In this experiment, a MCV – 1020 CNC machine tool made by Dah-Li Co. and a ψ0.3 mm micro end-mill were used to cut graphite. Ladder shape with 0.1mm step height was planned for machining. The machined workpiece is Fig.10. The measurement was made for the 0.6 mm-height step. The measured height is 0.6132 mm. Because the measurement accuracy is 0.0034 mm (the previous verification result), the machining depth error should be about 0.0098 mm (=0.0132-0.0034). To improve the machining accuracy, the depth error should be compensated to the machining NC program. With use of the compensated NC program, the machining accuracy can be further improved.

Fig.10 The machined ladder-shape workpiece

5. Conclusions

With use of integrating the image re-constructive algorithm, a depth measurement model and 2-step on-machine measurement method was proposed in this paper. The method eliminating the shadow effect caused by the light source can on-machine measure the micro depth error for error compensation by which the machining accuracy can be further improved. According to sensitivity analysis results, with the pixel resolution of 0.003 mm/pixel the measurement error $(\Delta b)_{\Delta C}$ can be controlled within ±0.0001 mm, if rotation error ΔC can be restricted within ±3°. Experimental results have also shown the effectiveness of the proposed method.

ACKNOWLEDGEMENT

This study is supported by National Science Council of the Republic of China under the grant number NSC 99-2221-E-033-048.

REFERENCES

1. P. Groombridge, A. Oloyede , P. Doherty-Bigara, "Development and implementation of visual feedback technology in automotive windscreen manufacture", Journal of Materials Processing Technology, 139 (2003), pp. 357–361.
2. Ajit S. Gaunekar, Gary P. Widdowson, Narasimalu Srikanth, Wang Guangneng, "Design and development of a high precision lens focusing mechanism using flexure bearings", Precision Engineering, 29 (2005), pp. 81–85.
3. Anjali V. Kulkarni, Madhuri G. Karnik, "Experimental Measurements and Theoretical Estimation of Temperature in ECDM Process", Proceedings of the 2004 International Conference on MEMS, NANO and Smart Systems (ICMENS'04).
4. J. Jurkovic, M. Korosec, J. Kopac, "New approach in tool wear measuring technique using CCD vision system", International Journal of Machine Tools & Manufacture, 45 (2005), pp. 1023–1030.
5. Johan Baeten, Joris De Schutter, "Hybrid Vision/Force Control at Corners in Planar Robotic-Contour Following", IEEE/ASME Transactions on Mechatronics, Vol. 7, No. 2, JUNE 2002.
6. Liangyu Lei, "A Machine Vision System for Bearing-diameter Inspecting", Proceedings of the 5th World Congress on Intelligent Control and Automation, June 15-19, 2004, Hangzhou, P.R. China.
7. P.F. Luoa, S.P. Pan, T.C. Chu, "Application of Computer Vision and Laser vision-based measurement method Interferometer to the Inspection of Line Scale", Optics and Laser vision-based measurement methods in Engineering, 42 (2004), pp. 563–584.
8. Kok-Meng Lee, Dehao Zhou, "A Real-Time Optical Sensor for Simultaneous Measurement of 3-DOF Motions", Proceedings of International Conference on Advanced Intelligent Mechatronics (AIM 2033).
9. Shih-Ming Wang, Han-Jen Yu, Yi-Hung Liu, Da-Fun Chen, Oct.15-18, 2007, "An on-machine error measurement system for micro-machining", ASME International Manufacturing Science and Engineering Conference.
10. J. F. Canny, "A computational approach to edge detection", IEEE Trans. Pattern Analysis and Machine Intelligence, 8(6):679-698, November 1986.